

# Peculiarities of Heat and Mass Transfer and Magnetohydrodynamic Processes Under Pulse Ionized Gas Rotation

V. N. Kharchenko  
N. P. Poluektov  
V. N. Zverev

Physics Department,  
Moscow Wood Technology Institute,  
Moscow, USSR

■ The characteristics of plasmas of hydrogen, helium, and argon, rotating in crossed fields of up to 80 kV/m and 0.8 T under a pulsed discharge in the stage of acceleration at powers ranging from 2 to 8 MW and in the stage of electric energy generation with a power of up to 60 MW, as well as in the regime of self-excited oscillations, are investigated experimentally. The electron concentration reaches  $5 \times 10^{21} \text{ m}^{-3}$ . The energy balance taking into account the heat flux to insulators is obtained, and a scheme of heat and mass transfer and magnetohydrodynamic processes in the case of self-excited oscillations is examined. The results can be used in the design and optimization of chemical plasma vortex devices, plasma centrifuges, and magnetohydrodynamic capacitors.

**Keywords:** *crossed electric and magnetic fields, energy balance, heat and mass transfer, heat flux, magnetohydrodynamic (MHD) processes, pulsed discharge, rotating plasma, self-excited oscillations*

## INTRODUCTION

Devices with rotating ionized gases have been studied to develop an efficient plasma chemical apparatus ensuring separation of the products obtained, a plasma centrifuge for isotope separation, and a magnetohydrodynamic (MHD) capacitor with regulated capacity [1, 2]. Experiments made on pulsed installations have revealed the following features of ionized gases rotating in crossed electric and magnetic fields [1]:

1. There are "plasma electrodes" along certain magnetic lines.
2. The angular velocity of a plasma is constant along each magnetic line.
3. The plasma rotation velocity does not exceed some critical value near insulators.
4. The magnetic field in a plasma expands and its strength decreases.
5. A fully ionized plasma without inhomogeneities of the spoke type is magnetohydrodynamically stable.
6. Particles are separated by mass.
7. The kinetic energy of a plasma is converted to a pulse of electric energy when the electrodes are short-circuited.

In this paper we offer new experimental information about ionized gases rotating in pulsed crossed fields. We describe the energy balance of such a gas, including the values of the heat flux to insulators, and indicate which processes of heat and mass transfer and MHD processes occur when the experimentally observed parameters undergo self-excited oscillations.

## EXPERIMENTAL ARRANGEMENT

The discharge chamber (Fig. 1) of the experimental installation consists of a steel cylinder 15 cm in radius provided with evacuation pipes and quartz flanges. Inside the chamber are two cathode rods of aluminum or molybdenum 2 cm in radius; two steel anode rings, connected with the cylinder shell; and two end quartz insulators separated by 54 cm. The main plasma region, 0.01 m<sup>3</sup> in volume, with a radial electric field to 80–140 kV/m, is bounded by "plasma electrodes" along the magnetic lines touching the electrode rods and rings. The ratio of the average radii in the central plane and near the insulators is  $r_0/r_H \approx 1.9$ . Four magnets in the form of coils, to which power is supplied from a capacitor battery, create an external magnetic field directed along the chamber axis with induction  $B_0 = 0.4\text{--}0.8$  T in the center and three times that value near the insulators. The discharge chamber was evacuated to a pressure of  $10^{-3}$  Pa. The working gas (hydrogen, helium, argon) is supplied by means of an electrodynamic valve whose piston pushes out a portion of gas to the chamber as a current pulse arises in the coils of the valve. The pulsed gas pressure in the chamber was measured by means of a pressure gauge according to the procedure described in Ref. 3. The gas pressure before a discharge,  $p_0$ , ranged from 2 to 15 Pa.

First, using ignitron Ig4, the magnets were powered from the battery C4 with a capacity of 18,000  $\mu\text{F}$  and a voltage of up to 5 kV, and the current in the magnets increased during 2 ms. Simultaneously, the capacitor C3 was discharged to the pulse valve coils, and a portion of the working gas was supplied to the chamber. After the entire chamber was filled

Address correspondence to Professor V. N. Kharchenko, Physics Department, Moscow Wood Technology Institute, 1-Institutskaya, 1, Mytishchi-1, Moscow, 14100, USSR

*Experimental Thermal and Fluid Science* 1990; 3:567-573  
© 1990 by Elsevier Science Publishing Co., Inc., 655 Avenue of the Americas, New York, NY 10010

0894-1777/90/\$3.50

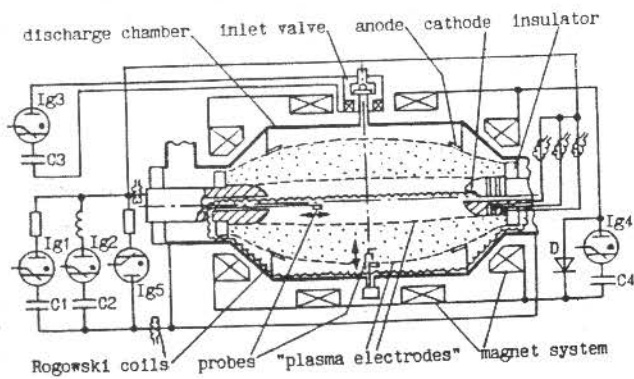


Figure 1. Experimental layout.

with the gas (over 1–2 ms), the pressure fell off exponentially with a time constant of 15–20 ms. When the voltage of battery C4 reversed its polarity, the currents in the magnets began to circulate through diodes D, and subsequently they decreased exponentially with a time constant of 20 ms. When the magnetic induction was maximum, the gas in the chamber was ionized by means of ignitron Ig1 from battery C1 with a capacity of 200  $\mu\text{F}$  and a voltage of up to 5 kV. After 100–200  $\mu\text{s}$ , using ignitron Ig2, the main battery C2, with a capacity of 600  $\mu\text{F}$  and a voltage of up to 10 kV, was discharged over a time of up to 500  $\mu\text{s}$ . By switching on ignitron Ig5, the plasma acceleration conditions were changed to those of energy generation with a pulse of induction current of the opposite direction over a time of about 10  $\mu\text{s}$ , over which the rotation of the plasma was stopped by the electromagnetic forces.

### MEASUREMENTS

In the course of these experiments, electrical, probe, and spectroscopic measurements of a complex of parameters in the various regions and at various stages of discharge have been made. The radial and azimuthal currents, voltage, and the profiles of the potential and of the induced magnetic field in the plasma were measured by using Rogowski coils (see Fig. 1), dividers, electrical probes, and magnetic probes, respectively, with the data recorded by memory oscillographs. From the oscillograms of voltage and discharge current obtained under the conditions of energy generation, the charge and the electric energy taken out of the plasma, as well as the equivalent capacity and average plasma mass density, were found. For diagnostic purposes, the cathode was made in the form of ring-shaped sections 0.4 cm wide with insulating disks of 0.3 cm each, the currents in each section being measured using the Rogowski coils.

During the spectroscopic measurements, the plasma radiation along the chord or axis of the chamber entered a spectrograph with a grating of 2400 marks/mm (a dispersion of 0.13 nm/mm). Using a dissector of a spectrum recorder, MRS-1, the contours of the spectral line under study were obtained at various moments of discharge (the contour scanning time 1–10  $\mu\text{s}$ ). The study of the lines during discharge was controlled by means of photomultipliers. The electron concentration was determined from the Stark half-width of the  $H_{\beta}$  line (to helium and argon, 0.1% of hydrogen was added). The electron temperature was found from the relative intensity of the lines due to argon or silicon ions (due to the erosion of the insulators)

and also the  $H_{\beta}$  and  $H_{\gamma}$  lines. The ion temperature was determined from the Doppler half-width of lines with the simple Zeeman effect [Ar II 480.6 nm, etc.], the  $\pi$  and  $\sigma$  components of which were isolated by using a Polaroid. The Doppler half-width of a component was found by taking into account the width due to the apparatus, which, according to the data obtained with a helium-neon laser, did not exceed 10% of the component half-width. The magnetic induction in the plasma was determined from the distance between the  $\sigma$  components of a line. The azimuthal ion velocity was found from the double Doppler shift of the line contours as the radiation went out in two opposite directions along the chord normal to the chamber axis.

### EXPERIMENTAL ERROR

The resolving power of the instrument made possible the determination of the minimum shift of a spectral line equal to 0.005 nm, corresponding to an error of 1.5 km/s in ion velocity. The number of experimental runs was enough to preclude the random error exceeding the systematic error. The relative error of ion velocity determination was within 15–20%. The relative errors of the spectroscopic measurements of the electron concentration and the magnetic field in the plasma were within the same limits. The relative errors in the measured values were as follows: electron temperature and ion temperature, 20–30%; currents and voltages, 5–10%; potential and induced magnetic field, 10–20%; equivalent capacity of the plasma, density of the generated electric energy, and heat flux to insulators, all within 25–35%.

These errors can be regarded as tolerable if one bears in mind the complexity, diversity, and very short duration of the processes involved, the large number and considerable variability of the parameters measured, and the fact that the errors do not exceed those of most experiments done with a rotating plasma [1]. The reliability of the results has been confirmed not only by the error determination but also by the allowable spread of the data obtained in numerous repeated runs and in measuring by different methods, as well as by obtaining all known features of a rotating plasma listed in the Introduction.

### ELECTRICAL CHARACTERISTICS

Typical oscillograms of the voltage and radial current in the plasma in the case when the power is supplied by a single battery through a resistor are shown in Fig. 2, and those obtained in the case of power supplied by two batteries through

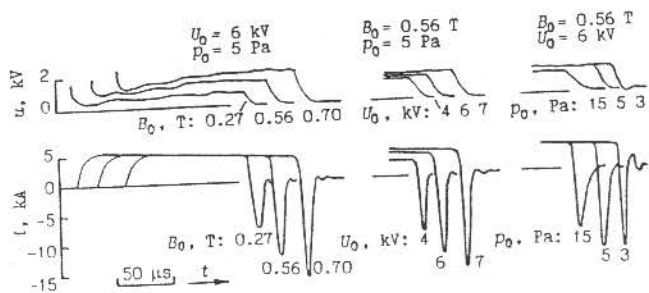


Figure 2. Oscillograms of voltage  $u$  and current  $i$  of discharge in argon at the various values of magnetic field  $B_0$ , capacitor voltage  $U_0$ , and initial pressure  $p_0$ .

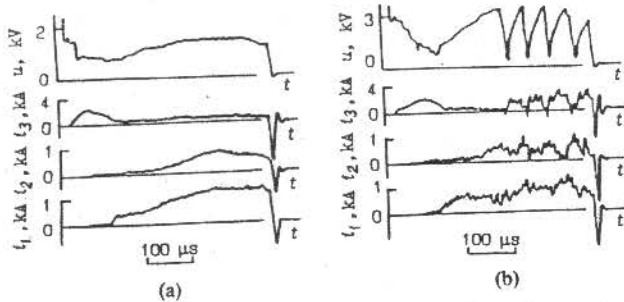


Figure 3. Oscillograms of discharge voltage  $U$  and currents in cathode sections  $i_k$  for hydrogen at two values of magnetic field  $B_0$ . (a)  $B_0 = 0.42$  T; (b)  $B_0 = 0.65$  T.

an inductance coil are presented in Fig. 3. Under the plasma acceleration conditions, the discharge power reached 2–8 MW at a radial current up to 2–5 kA. From Fig. 4a one can notice that the experimental values of the discharge voltage  $U$  in the quasi-stationary phase of plasma acceleration coincide with the values calculated by means of the formula [1]

$$U = \epsilon v_c B_0 (r_2 - r_1) r_0 / r_H \quad (1)$$

where  $v_c$  is the critical velocity,  $v_c = (2E_i/m)^{1/2}$ ,  $m$  and  $E_i$  being the mass and ionization energy of an atom;  $B_0$  is the external magnetic field in the center;  $r_2$  and  $r_1$  are the radii of the "plasma electrodes" in the central plane;  $r_0$  and  $r_H$  are the average radii of the plasma in the central plane and near the insulators; and  $\epsilon = 1$  for hydrogen and helium,  $\epsilon = 3$  for argon. Assuming  $U = \langle v_\phi \rangle B_0 (r_2 - r_1)$  for the measured  $U$  values in hydrogen, we obtain the average plasma velocity  $\langle v_\phi \rangle = 80$  km/s in the central plane and 50 km/s near the insulators.

Under the conditions of electric energy generation with induced reverse current of up to 20 kA and a power of up to 60 MW, an electric energy output of 200–300 J was obtained from the rotating plasma. The experimental values of the generated electric energy  $W$  and the equivalent capacity  $C$  of the rotating plasma (an MHD capacitor) turned out to be directly and inversely proportional, respectively, to the magnetic field  $B_0$  (see Fig. 4b). To the measured values of  $C$  there correspond the average values of ion concentration

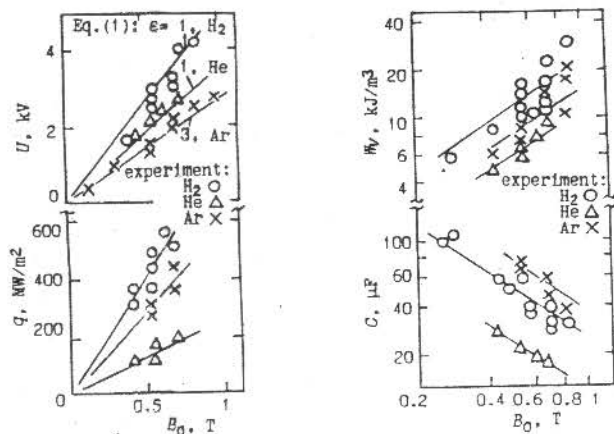


Figure 4. Discharge voltage  $U$ , heat flux to insulators  $q$ , generated energy  $W$ , and equivalent capacity  $C$  for the various gases as a function of magnetic field  $B_0$ . (Note: Straight lines indicate calculations according to Eq. (1) with different  $\epsilon$ .)

$\langle n_i \rangle = (2.5) \times 10^{21}$ ,  $(0.5-1) \times 10^{21}$ , and  $(0.4-1) \times 10^{21} \text{ m}^{-3}$  for hydrogen, helium, and argon, respectively, which have been found by the formula [1]

$$\langle n_i \rangle = C B_0^2 (r_2 - r_1)^2 / V m_i \quad (2)$$

where  $C$  is the equivalent capacity of a rotating plasma,  $V$  is the volume of the main region of the plasma, and  $m_i$  is the ion mass. The above values of  $\langle n_i \rangle$  correspond to the values of energy  $W$  near its maximum and are directly proportional to the field  $B_0$ . When the working gas pressure  $p_0$  before a discharge was considerably lower or higher than the value corresponding to these values of  $\langle n_i \rangle$ , the generated energy  $W$  decreased (see Fig. 2,  $p_0 = 15, 5$ , and 3 Pa).

## RESULTS OF PROBING MEASUREMENTS

Using electrical probes in the region of the "plasma anode," the potential oscillations with a frequency of 0.1–1 MHz and an amplitude up to 10–30 V, which arose as the plasma was rotating, were recorded. In the nonrotating plasma at  $B_0 > 0$  (after electric power generation), and at a discharge with  $B_0 = 0$ , no potential oscillations were observed. As the plasma rotated faster and faster, the radial profile of the potential in the central plane (at  $z = 0$ ), and therefore the "plasma anode," were displaced toward the periphery by  $\Delta r_2 = 0.2-0.8$  cm (Fig. 5a). According to Lehnert [1], such a shift corresponds to the following ratio of centrifugal pressure to magnetic pressure:

$$\beta_c = 2\mu_0 \frac{(r_2 - r_1)\rho v_\phi^2}{r_0 B^2} = 4 \frac{\Delta r_2}{r_2} = 0.09-0.35$$

where  $\rho$  is the plasma mass density,  $v_\phi$  is the rotation velocity, and  $\mu_0$  is the permeability of vacuum. From Fig. 5a it can be seen that in the peripheral region at  $r > 9-10$  cm the floating potential  $\varphi_f$  exceeds the potential of the anode rings and that of the shell,  $\varphi_A$ . The experimental values  $\varphi_f - \varphi_A$ , which reach 40–60 V, are due to the Faraday component of the radial electric field  $v_\phi B$ . Both the results of our calculations and the measured values of the speed of propagation of signals between two probes displaced azimuthally suggest that the plasma velocity  $v_\phi$  in the peripheral region should be rather high. The above speeds were equal to 27, 15, and 6.5 km/s at  $r = 8, 9$ , and 10 cm, respectively, at 300  $\mu\text{s}$  after the onset of a discharge in hydrogen and with  $B_0 = 0.56$  T. In the region  $r < 7.5$  cm, no electrical probe measurements were made because the character of the discharges was different there.

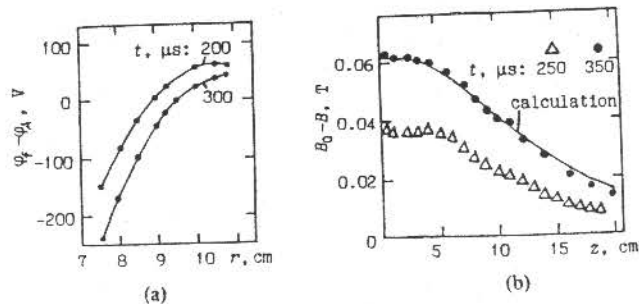


Figure 5. Experimental profiles of (a) floating potential  $\varphi_f(r) - \varphi_A$  in the central plane ( $z = 0$ ) and (b) induced magnetic field  $B_0 - B(z)$  on the axis ( $r = 0$ ) for hydrogen at various moments  $t$  of discharge.

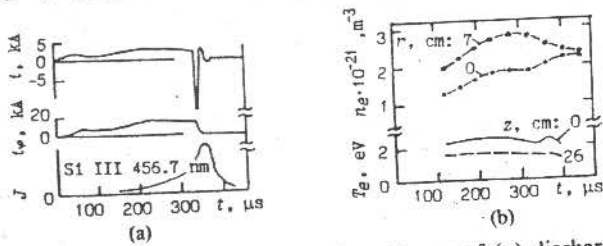


Figure 6. Experimental temporal dependences of (a) discharge current  $i$ , azimuthal current  $i_\phi$ , silicon ion radiation intensity  $J$  and (b) electron concentration  $n_e$  and electron temperature  $T_e$  for hydrogen at  $B_0 = 0.56$  T.

From oscillograms obtained with magnetic probes, the induced magnetic field  $B - B_0$  due to the flow of the azimuthal current in the plasma was measured. As the current in the plasma disappeared and the plasma stopped rotating (after some electric energy was generated), the induced magnetic field also vanished. In the peripheral region, magnetic field oscillations in the plasma with an amplitude up to 0.05 T and a frequency between 0.1 and 1 MHz were observed; there were no magnetic field oscillations at  $r = 0$ . The measurements along the radius for the case of the maximum change in magnetic field when a discharge occurs in hydrogen yield the following ratios of the magnetic field value in the plasma to that of the external field,  $B/B_0 = 0.81, 0.86, 1.0,$  and  $1.1$  at  $r = 0, 7.5, 9,$  and  $11$  cm, respectively. The induced magnetic field profiles along the chamber axis at  $r = 0$ , which were measured at various moments of a discharge in hydrogen at  $B_0 = 0.42$  T, are illustrated in Fig. 5b. The experimental distribution of  $B - B_0 = f(z)$  in the regime of quasi-stationary plasma rotation agrees with the calculated magnetic field profile due to an azimuthal current of 14 kA in the main region of the plasma. According to the oscillograms, the total azimuthal current in the discharge chamber increased as the plasma was accelerated up to 13–18 kA, and it fell off to zero when the plasma stopped rotating (Fig. 6a,  $i_\phi$ ).

### MEASUREMENTS WITH A SECTIONALIZED CATHODE

From the current oscillograms in the various sections of the cathode (Fig. 3a), it can be seen that the discharge started at the center of the discharge chamber (as the value of the current  $i_3$  from the half containing the main plasma region is large). As the plasma was accelerated, current  $i_3$  practically disappeared, while currents  $i_2$  and  $i_1$  from the layers near the insulator increased, so that under the quasi-stationary conditions the current densities on the cathode sections became  $j_1 \approx j_2 \ll j_3$  (Fig. 7a). Such a discharge-current distribution

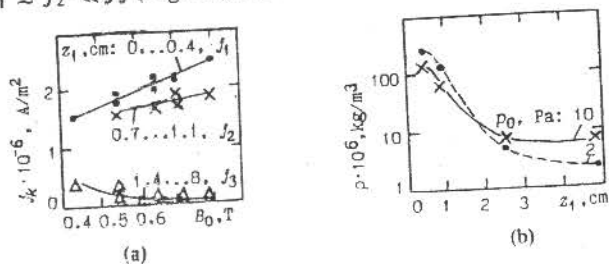


Figure 7. Experimental dependency (a) of current density  $j_k$  on cathode sections upon magnetic field  $B_0$  and (b) of plasma mass density  $\rho$  upon distance from insulator ( $z_1$ ) for hydrogen.

with an increased current density near the insulators is the distinguishing feature of a Hartmann flow, whose properties are acquired by a vortex plasma flow in crossed fields  $E_r$  and  $B_z$ . In the experiment, as the magnetic field  $B_0$  increased, the current density  $j_1$  (near the insulator) grew and the value of  $j_3$  decreased. To the experimental values of currents  $i_1, i_2,$  and  $i_3$  and the current densities  $j_1, j_2,$  and  $j_3$  under the quasi-stationary discharge conditions in hydrogen at  $B_0 = 0.42$  T, there correspond the average densities of the radial current in the plasma ( $\langle j_r \rangle = 900 \pm 200$  and  $450 \pm 150 \text{ kA/m}^2$  at distances  $z_1 = 0-0.55$  and  $0.55-1.25$  cm from the insulator and  $\langle j_r \rangle = 7 \pm 2 \text{ kA/m}^2$  in the main plasma region, which is in accord with the calculated profile of  $j_r(z)$  [4].

With the sectionalized cathode, a rotating plasma displays the properties of parallel capacitors with  $C_k, V_k,$  and  $\rho_k$  values corresponding to the  $k$ th section and to Eq. (2), where  $\rho_k$  is the mass density of the  $k$ th section of the plasma:  $\rho_k = \langle m_i n_i \rangle_k$ . The values of  $C_k$  necessary for determining  $\rho_k$  were found from the current and voltage oscillograms for the  $k$ th section taken under the electric energy generation conditions (see Fig. 3a). Plasma mass densities versus distance from the insulator are plotted in Fig. 7b. The high densities near the insulator are caused by its erosion.

For a discharge in hydrogen in the case of quartz insulators, magnetic field  $B_0 \geq 0.65$  T, and discharge voltage  $U \geq 3$  kV ( $t \geq 250 \mu\text{s}$  from onset), the phase of the steady acceleration of the plasma suddenly changed to new conditions characterized by sawtooth oscillations of the voltage (from  $U$  to  $\sim 0$ ) and the current in the main region (with brief reversals of current direction) with a period of about  $50 \mu\text{s}$  (see Fig. 3b). The emergence of these self-oscillations was significantly affected by the insulator material but not by the electrode material. For cathodes made of molybdenum, aluminum, copper, and steel, the obtained discharge characteristics were practically the same. If, however, organic glass was used instead of quartz as the insulator material, this resulted in a decrease in the voltage observed just before the self-oscillations by a factor of 2–3. Under the conditions of self-oscillation, the intensity of the spectral line due to silicon ions increased dramatically, suggesting enhanced erosion of the quartz insulator.

### RESULTS OF SPECTROSCOPIC MEASUREMENTS

In the experiment, the line spectrum due to the ions Ar II and Ar III (working gas) and also to those of Si II, Si III, Si IV, and O II (resulting from the erosion of quartz) was mainly observed, thus testifying to a strong ionization of the plasma (see  $J$ , Fig. 6a). The measurements show that the electron concentration in the central plane at  $r = 7$  cm is a factor of 1.5 or more as high as that at the axis. When the electric energy generation and plasma rotation came to an end, the electron concentration values at  $r = 0$  and 7 cm became equal over a time of about  $150 \mu\text{s}$  (see  $n_e$ , Fig. 6b). The results of the spectroscopic measurements of electron concentration are within the range of concentration values obtained from the current and voltage oscillograms under the energy generation conditions.

The electron temperature was 2–3 eV (see  $T_e$ , Fig. 6b, where the  $z = 26$  cm curve is obtained from the lines due to Si II 505.6 and 385.6 nm in the vicinity of the insulator and the  $z = 0$  curve is obtained from the lines due to Si IV 411.6 and 421.2 nm in the main region). According to Boldyrev et al [5], the temperature of the ions of Ar II and Ar III (the working

gas) was 7-12 eV and 13-15 eV, respectively, the temperature of the ions of Si II and Si III at a discharge in hydrogen having approximately the same values. The magnetic induction values found from the distances between the  $\sigma$  components of the lines coincide with the magnetic probe data.

For a discharge in argon at a pressure  $p_0 = 4-5$  Pa and magnetic field  $B_0 = 0.7$  T, the azimuthal velocity of the ions of Ar II and Ar III in the central plane equaled 18-22 km/s and 23-27 km/s, respectively. At a constant angular velocity of the plasma along the magnetic line, the plasma rotation velocity near the insulator is  $r_0/r_H$  times as low and is equal to  $(1.1-1.6)v_c$ , where  $v_c = 8.7$  km/s is the critical velocity for argon. At the above-mentioned values of  $p_0$  and  $B_0$  in the central plane, the ratio of the kinetic energy of the azimuthal motion of Ar II and Ar III ions to their temperature was found to be  $m_i v_\phi^2 / 2T_i = 7-9$  and 8-10, respectively [5]. For a discharge in hydrogen, the azimuthal velocities of the ions of Si II, Si III, and Si IV resulting from quartz erosion ranged from 10 to 40 km/s. As the magnetic field decreased and the initial gas pressure increased, the ion velocities decreased.

### ENERGY BALANCE

In order to establish the principal channels of distribution of the electric energy produced and the features of the process of heat transfer, as well as to determine the fraction of the heat flow rate due to the electric power supplied to the boundary layer to the insulator, we have calculated the components of the energy balance, the scheme of which is presented in Fig. 8. In the main volume of the plasma and in the two boundary layers near the insulators, this balance obeys Ohm's generalized law multiplied by the current density, the equation of motion multiplied by the velocity, and the energy equation. These equations can be written in the form [1, 6]

$$IU = N_A + D, \quad K_z = N_p + N_A - N_\eta, \\ H_z + K_z = IU + N_{\eta z} - Q \quad (3)$$

where  $IU$  is the electric power supplied to the plasma;  $N_A, N_p, N_\eta$  are the work done per second by the Ampere forces, pressure, and viscosity, respectively;  $N_{\eta z}$  is the work done by the viscous stress on the surface of the boundary separating the main and end boundary regions;  $K_z$  and  $H_z$  are the transfer rates of kinetic energy and enthalpy through the boundary between the regions (these rates are due to the secondary circulation of the plasma in the meridian plane of the channel);  $D$  is the Joule dissipation;  $Q$  is the heat flow rate from the region under consideration; and

$$N_A = \int_V \mathbf{v}(\mathbf{j} \times \mathbf{B}) dV, \quad D = \int_V \frac{j^2}{\sigma} dV,$$

$$N_\eta = - \int_V \mathbf{v} \operatorname{div} \hat{\sigma} dV$$

$$N_{\eta z} = \oint_S \sum_\alpha \sigma_{n\alpha} v_\alpha dS, \quad H_z = \oint_S (\rho u + p) v_n dS$$

where  $\hat{\sigma}$  is the viscous stress tensor;  $\sigma$  the conductivity,  $\rho$  the mass density,  $p$  the pressure, and  $u$  the specific internal energy of the plasma; and  $j$  is the current density.

The energy balance in each region of the channel (the main region and the boundary regions) is also described by the following formulas for the enthalpy transfer rate  $H_z$ , the viscous

dissipation  $\Phi$ , and the energy equation in a second form [1, 6]:

$$H_z = U_z + N_p - N_\rho, \quad \Phi = N_\eta + N_{\eta z}, \\ U_z = -N_\rho + D + \Phi - Q \quad (4)$$

where  $U_z$  is the internal energy transfer rate through the boundary between the regions, and  $N_\rho$  is the work done by the expanding plasma:

$$N_\rho = \int_V p \operatorname{div} \mathbf{v} dV.$$

For the heat flow rate  $Q$  from each region and for the heat flow rate  $Q_w$  flowing to the walls of the respective channel region (anode, cathode, insulator, and chamber shell), we can write

$$Q = Q_k + Q_r = Q_w + Q_{kz} + Q_{rz} \\ Q_w = Q_A + Q_K + Q_{in} + Q_t \quad (5)$$

where  $Q_k, Q_r, Q_{kz}, Q_{rz}$  are the convection and radiation heat flow rates from the region under consideration and the heat flow rates through the boundary between the regions.

The initial electric powers of the balance  $I_0 U$  and  $I_H U$ , supplied to the main region and to the boundary regions under quasi-stationary discharge conditions, were measured by using the oscillograms taken for the individual cathode sections (see Fig. 3a). The values of the balance constituents, indicated in the scheme of Fig. 8, were tentatively estimated from the measured values of the radial and azimuthal currents, electron concentration and temperature, ion temperature and velocity, the profiles of the potential and the velocity near the "plasma anode," and the plasma mass density in the boundary layer given above. We also took into account the velocity current density profiles obtained from Ref. 4. The calculations were made using the formulas for the absolute or relative values of the balance components, making use of the classical transfer coefficients [1] and confirming that the individual balance relations (3)-(5) hold in each region of the channel.

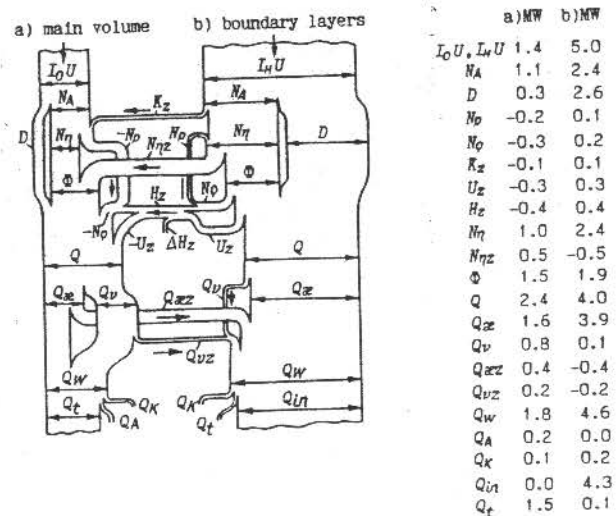


Figure 8. Scheme of the energy balance and values for its components (tabulated on the right, in MW) (a) in the main plasma volume and (b) in the two boundary layers for hydrogen at  $B_0 = 0.42$  T.

**Table 1.** Conditions for Insulators in Two Plasma Installations

| Parameter                                | MHD<br>U-25 [7] | Pulsed<br>(Fig. 1) |
|--|-----------------|--------------------|
| Main plasma volume $V$ (m <sup>3</sup> ) | 2.8             | 0.01               |
| Generated power $P$ (MW)                 | 12              | 60                 |
| Magnetic field $B$ (T)                   | 2               | 2                  |
| Electric field $E$ (kV/m)                | 2               | 140                |
| Plasma velocity $v$ (km/s)               | 1               | 50                 |
| Heat flux $q$ (MW/m <sup>2</sup> )       | 2               | 500                |

### RATE OF HEAT FLOW TO INSULATORS

The measured electric power supplied in the main and boundary regions under the quasi-stationary conditions at  $B_0 = 0.42$  T in hydrogen was 1.4 and 5.0 MW, that is, 22 and 78% of the total electric discharge power of 6.4 MW. According to the balance data (see Fig. 8), the rate of heat flow into the walls of the two end-face insulators amounted to 4.3 MW, that is, 86% of the power in the boundary layers  $I_H U$ . The relatively small value of the total energy transfer rate through the boundary between the regions (14% of  $I_H U$ ) made it possible to find, from the measured electric power in the boundary layer, the average heat flux to the insulator,  $q$ , using the relation

$$q = a I_H U / 2S \quad (6)$$

where  $I_H/2 = I_1 + I_2$  is the current strength in two cathode sections near one insulator (and in the boundary layer) in the quasi-stationary acceleration phase (see Fig. 3a),  $U$  is the voltage,  $S$  is the area of the working surface of the insulator, and  $a$  is the fraction of the electric power in the boundary layer that eventually goes to the insulator.  $a = 0.86$  for the above parameters and lies within 0.8–0.9 for other discharge parameters.

The results of this indirect measurement of the heat flux to insulators are illustrated in Fig. 4a. The values of  $q$  turned out to be proportional to the magnetic field  $B_0$ ; at  $B_0 = 0.70$  T,  $q = 500, 200,$  and  $400$  MW/m<sup>2</sup> for hydrogen, helium, and argon, respectively.

Table 1 compares thermal and electrical loads on the insulators in a stationary MHD installation (designated U-25) [7] and in the pulsed installation being considered.

Because of such extreme loads in the present discharge, the strong spectral lines due to Si II, Si III, Si IV, and O II (resulting from the erosion of insulators), as well as sawtooth oscillations of voltage and current (caused by electrical breakdowns of the insulator, the material of which significantly affected the parameters of the transition to oscillations) were observed.

### HEAT AND MASS TRANSFER AND MHD PROCESSES IN THE CASE OF SELF-EXCITED OSCILLATIONS

The above-mentioned peculiarities and parameters of a rotating plasma, the thermal and electrical loads on insulators, and also the character of the oscillograms (see Fig. 3b) correspond to the following scheme of interrelated processes of heat and mass transfer and of magnetohydrodynamics in the present discharge in the case of self-excited parameter oscillations [8].

As the plasma rotation velocity increases under the acceleration conditions, the voltage between the electrodes, the fraction of the discharge current near the insulators, the heat flux to the insulators, and the temperature, surface conductivity, and erosion rate of the insulators all increase. The erosion products diffuse, assisted by the ionization processes, into the rotating plasma, thereby changing its parameters. In a high electric field  $E$  of about 100 kV/m, on the heated insulators with a surface conductivity  $\sigma\delta$  of more than 0.05 S (in the stationary MHD installation U-25,  $\sigma\delta = 0.7$  S [7]), there arises a surface source of heat with a heat flux  $q_s = \sigma\delta E^2 \geq 500$  MW/m<sup>2</sup>, which, together with the heat flux  $q$  from the plasma, heats up each insulator until an electrical breakdown occurs in one of them. As the breakdown takes place, the plasma acceleration conditions change to those of electric energy generation with the reverse induction current. The reversed electromagnetic forces rapidly stop the plasma rotation, and the voltage, the heat flux to the insulators, and their temperature and surface conductivity all drastically decrease. The dielectric properties of the insulator in which the breakdown occurred are then restored, which signifies the beginning of the next cycle of plasma acceleration, with the above processes again occurring.

A mathematical model of these interdependent nonstationary processes was developed in Ref. 8, and the calculated self-excited oscillations dependence of voltage upon time has been confirmed by the experimental oscillogram.

### PRACTICAL SIGNIFICANCE

The results obtained and the comparison with the stationary MHD installation U-25 indicate that it is expedient to simulate heat and mass transfer and magnetohydrodynamic and other processes taking place in stationary plasma chemical vortex installations and plasma centrifuges by using the developed pulsed installation. This would make relevant studies both rapid and economical over a wide range of parameters, including conditions of overload and emergency.

The data presented here correspond to parameters of vortex-plasma devices at the specific power of discharge in the range 200–800 MW/m<sup>3</sup>. The measured high values of the ratio  $m_i v_p^2 / 2T_i = 7-10$  indicate that these devices are highly effective in separating products or isotopes.

The established dependencies also represent characteristics of a magnetohydrodynamic vortex-plasma capacitor intended to provide intense electric energy pulses upon plasma acceleration. The specific energy of such a capacitor (per kilogram of working gas) is quite high, up to  $3 \times 10^9$  J/kg. The recommended working gases are hydrogen and argon.

The results show how the thermal stability and electrical strength of the end-face insulators limit the discharge parameters in the above-mentioned technological and power-producing rotating plasma devices. For these devices, a new stage of discharge—that of self-excited oscillations leading to periodic breakdowns of an insulator followed by restoration of its electrical strength—has been established.

### CONCLUSIONS

The characteristics of hydrogen, helium, and argon plasmas rotating as a result of a pulsed discharge in crossed fields up to 80 kV/m and 0.8 T have been studied experimentally. In the

stage of plasma acceleration at powers between 2 and 8 MW, the electron concentration and temperature reached  $5 \times 10^{21} \text{ m}^{-3}$  and 2–3 eV, the temperature of the Ar II and Ar III ions and the azimuthal velocity of these ions were 7–15 eV and 18–27 km/s, and the induced magnetic field and azimuthal current were as high as 0.06 T and 18 kA. With increasing distance from the insulator toward the main plasma region, the radial current density dropped from 900 to 7 kA/m<sup>2</sup>, the floating potential outside the "plasma anode" exceeding the anode potential by 40–60 V. When the electrodes were short-circuited, the electric energy output reached 200–300 J at a power of 60 MW. A new stage of discharge, characterized by sawtooth self-excited oscillations of voltage and other parameters, has been described.

The energy balance in the main and boundary plasma regions was obtained. The thermal and electrical loads on the quartz insulators reached 500 MW/m<sup>2</sup> and 140 kV/m, respectively. A scheme for the heat and mass transfer and magnetohydrodynamic processes in the case of self-excited parameter oscillations was discussed.

The results presented here can be used to develop and optimize efficient plasma-vortex chemical devices, plasma centrifuges, and MHD capacitors.

### NOMENCLATURE

|          |  |
|----------|--|
| <i>a</i> | coefficient, dimensionless   |
| <i>B</i> | magnetic induction, T  |
| <i>C</i> | equivalent capacity of a rotating plasma, F                              |
| <i>D</i> | Joule dissipation, W   |
| <i>E</i> | electric field strength, V/m   |
| <i>H</i> | enthalpy transfer rate, W  |
| <i>I</i> | electric current strength in the quasi-stationary phase, A               |
| <i>i</i> | electric current strength, A   |
| <i>j</i> | electric current density, A/m <sup>2</sup>                               |
| <i>K</i> | kinetic energy transfer rate, W  |
| <i>m</i> | atomic mass, kg  |
| <i>N</i> | power due to a force, W  |
| <i>n</i> | particle concentration, m <sup>-3</sup>                                  |
| <i>P</i> | generated electric power, W  |
| <i>p</i> | pressure, Pa   |
| <i>Q</i> | heat flow rate, W  |
| <i>q</i> | heat flux density, W/m <sup>2</sup>                                      |
| <i>r</i> | radial coordinate or average radius, m                                   |
| <i>S</i> | area, m <sup>2</sup>   |
| <i>T</i> | particle temperature, eV   |
| <i>t</i> | time, s  |
| <i>U</i> | internal energy transfer rate, Eq. (4), W                                |
| <i>U</i> | voltage between the electrodes in the quasi-stationary phase, Eq. (1), V |
| <i>u</i> | voltage between the electrodes, V  |
| <i>V</i> | volume of the main region, m <sup>3</sup>                                |
| <i>v</i> | velocity, m/s  |
| <i>W</i> | generated electric energy, J   |
| <i>z</i> | longitudinal coordinate, m   |

### Greek Symbols

|           |   |
|-----------|---|
| $\beta_c$ | centrifugal to magnetic pressure ratio, dimensionless |
|-----------|---|

|                |                                   |
|----------------|-----------------------------------|
| $\epsilon$     | coefficient, dimensionless        |
| $\mu_0$        | permeability of vacuum, H/m       |
| $\rho$         | mass density, kg/m <sup>3</sup>   |
| $\sigma$       | plasma conductivity, S/m          |
| $\sigma\delta$ | insulator surface conductivity, S |
| $\Phi$         | viscous dissipation, W            |
| $\varphi$      | electric potential, V             |

### Subscripts

|               |   |
|---------------|---|
| <i>A</i>      | Ampere forces; anode                                |
| <i>c</i>      | critical  |
| <i>e</i>      | electron  |
| <i>f</i>      | floating  |
| <i>H</i>      | boundary layers                                     |
| <i>i</i>      | ion   |
| <i>in</i>     | insulator   |
| <i>K</i>      | cathode   |
| <i>p</i>      | pressure  |
| <i>r</i>      | radial component                                    |
| <i>t</i>      | shell   |
| <i>w</i>      | wall  |
| <i>z</i>      | boundary between main and end-face boundary regions |
| 0             | main region   |
| $\kappa$      | convective  |
| $\nu$         | radiative   |
| $\eta$        | viscous force                                       |
| $\varphi$     | azimuthal component                                 |
| 1             | plasma cathode                                      |
| 2             | plasma anode  |
| $k = 1, 2, 3$ | sections of cathode and parts of plasma             |

### REFERENCES

- Lehnert, B., Rotating Plasmas, *Nucl. Fusion*, **11**, 485–533, 1971.
- Rusanov, V. D., and Fridman, A. A., *Physics of Chemically Active Plasmas*, Nauka, Moscow, 1984.
- Andryukhina, E. D., Measurement of Pulsed Pressure, *Prib. Tekhn. Eksp.*, N1, 202–204, 1961.
- Zverev, V. N., Longitudinal Velocity Distributions in Rotating Plasmas, *Zhurnal Tekhn. Fiziki*, **54**(12), 2289–2296, 1984.
- Boldyrev, V. R., Poluektov, N. P., and Kharchenko, V. N., Experimental Study of the Dynamics of Processes in a Pulsed Plasma Centrifuge, *Sov. Plasma Phys.*, **11**(4), 425–429, 1985.
- Landau, L. D., and Lifshitz, E. M., *Electrodynamics of Continuous Media*, Nauka, Moscow, 1982.
- Beilis, I. I., Bityurin, V. A., Vasilieva, I. A., Kirillov, V. V., Koryagina, G. M., Lyubimov, G. A., Medin, S. A., Morozov, G. N., Sheindlin, A. E., and Shumyatsky, B. Ya., *Magnetohydrodynamic Energy Conversion, Physical and Engineering Aspects*, Nauka, Moscow, 1982.
- Zverev, V. N., and Kharchenko, V. N., Heat and Mass Transfer in Devices with Pulsed Rotation of an Ionized Gas, Reports for the Minsk International Forum on Heat and Mass Transfer, Minsk, ITMO AN BSSR, Sec. 11, pp. 43–45, 1988.